Contribution from the Department of Chemistry,
University of Minnesota, Minneapolis, Minnesota 55455

Heterobimetallic Au–Os and Au–Ru Hydrido Complexes. X-ray Crystal and Molecular Structures of $[Au_2Os(H)_3(PPh_3)_5]PF_6$ and $[AuRu(H)_2(CO)(PPh_3)_4]PF_6$

Bruce D. Alexander, M. Pilar Gomez-Sal,† Patrick R. Gannon, Christine A. Blaine, Paul D. Boyle, Ann M. Mueting, and Louis H. Pignolet*

Received March 16, 1988

Several new heterobimetallic hydrides containing gold have been synthesized. $[Au_2Os(H)_3(PPh_3)_5]PF_6$ (**1**) was made by the reaction of $AuPPh_3NO_3$ and $Os(H)_4(PPh_3)_3$ with CH_2Cl_2 as solvent. $[Au_2Ru(H)_3(PPh_3)_5]PF_6$ (**2**) was synthesized in an analogous manner from $AuPPh_3NO_3$ and $Ru(H)_4(PPh_3)_3$ with toluene as solvent. $[AuRu(H)_2(CO)(PPh_3)_4]PF_6$ (**3**) and its osmium analogue, $[AuOs(H)_2(CO)(PPh_3)_4]PF_6$ (**4**), and $[AuOs(H)_2(CO)_2(PPh_3)_3]PF_6$ (**5**) and its ruthenium analogue, $[AuRu(H)_2(CO)_2(PPh_3)_3]PF_6$ (**6**), were prepared by the reaction of $AuPPh_3NO_3$ with $M(H)_2(CO)(PPh_3)_3$ (M = Ru, Os) and $M(H)_2(CO)_2(PPh_3)_2$ (M = Ru, Os), respectively, with CH_2Cl_2 as solvent. Compounds **1** and **3** were characterized by single-crystal X-ray diffraction in the solid state [**1**·$3CH_2Cl_2$·$2Et_2O$, monoclinic $P2_1/n$, a = 13.64 (2) Å, b = 40.89 (2) Å, c = 17.53 (1) Å, β = 102.54 (9)°, T = −116 °C, Z = 4, R = 0.051 for 10 180 observations; **3**·$2CH_2Cl_2$, triclinic $P\bar{1}$, a = 15.404 (3) Å, b = 19.461 (8) Å, c = 13.868 (7) Å, α = 98.86 (4)°, β = 105.68 (3)°, γ = 87.73 (2)°, T = 22 °C, Z = 2, R = 0.051 for 9648 observations] and by ^{31}P and ^1H NMR spectroscopy in solution. The structure of complex **1** consists of two $Au(PPh_3)$ units bonded to an $Os(PPh_3)_3$ moiety forming a slightly distorted trigonal-bipyramidal geometry with no Au–Au bond (4.28 Å). The hydride ligands were not directly observed by X-ray diffraction in **1**; however, spectroscopic evidence indicates the presence of one hydride bridging each of the Au–Os bonds on the outside edges of the Au_2Os triangle and a third hydride briding one of the Au–Os bonds on the inside edge of the Au_2Os triangle. Supporting evidence for the characterization of complex **1** in the solid state was obtained with the use of CP MAS ^{31}P NMR spectroscopy. In the X-ray diffraction analysis of complex **3** one of the hydride ligands was directly observed bridging the Au–Ru bond. Spectroscopic evidence supports the formulation of **3** as a bis(μ-hydrido) species. The average Au–Os and Au–Ru distances in **1** and **3** are 2.703 (0) and 2.786 (1) Å, respectively, and the Ru–H and Au–H separations in **3** are 1.78 (4) and 1.61 (4) Å, respectively. Compounds **2** and **4–6** were also determined to have bridging hydrides by NMR and IR spectroscopy. Preliminary results indicate that the gold adduct $[AuRu(H)_2(CO)(PPh_3)_4]PF_6$ (**3**) has a significantly higher rate of catalytic activity than its parent complex, $Ru(H)_2(CO)(PPh_3)_3$, for the isomerization of 1-hexene to *cis*- and *trans*-2-hexene in CH_2Cl_2 at 25 °C and 1 atm of N_2.

Introduction

The synthesis, structural characterization, and reactivity studies of mixed transition-metal–gold cluster compounds are rapidly expanding fields of study.[1-36] These compounds are important not only because of their novel structural properties and their potential for assisting in understanding the role of gold in bimetallic surface catalysis,[37-41] but also because of their potential as homogeneous bimetallic catalysts. Of the cluster compounds synthesized to date, however, only a few have shown catalytic behavior under homogeneous conditions.[38,42,43] It is our goal to continue to synthesize and characterize new transition-metal–gold cluster compounds and to study their reactivities, especially as they relate to catalysis, in an effort to develop a better understanding of the role of gold in catalysis.

A variety of transition-metal–gold hydride cluster compounds have been prepared in our laboratory over the past several years.[1-10] Recently, we reported the synthesis, single-crystal X-ray analysis, and spectroscopic characterization of several gold–ruthenium hydride cluster compounds.[2,4,5] We have made further progress in this area and have extended it to the synthesis of gold–osmium complexes. $[Au_2Os(H)_3(PPh_3)_5]PF_6$ (**1**), $[AuOs(H)_2(CO)(PPh_3)_4]PF_6$ (**4**), and $[AuOs(H)_2(CO)_2(PPh_3)_3]PF_6$ (**5**) were synthesized along with their ruthenium analogues. Compound **1** and the ruthenium analogue of **4**, $[AuRu(H)_2(CO)(PPh_3)_4]PF_6$ (**3**), were characterized by single-crystal X-ray diffraction and by ^{31}P and ^1H NMR spectroscopy. Complex **1** was also characterized by CP MAS ^{31}P NMR spectroscopy. The hydride ligands in **1** were not located by X-ray diffraction, and only one hydride ligand was directly observed in the molecular structure of **3**. Spectroscopic evidence indicates, however, that all six complexes have hydrides bridging the Au–M bonds. Complex **1** is unusual in that there is no Au–Au bonding interaction. This is due to the presence of a hydride ligand bridging one of the Au–Os bonds and located between the two gold atoms in the Au_2Os plane. The gold–ruthenium cluster compound **3** shows a significant increase in the rate of isomerization of 1-hexene to *cis*- and *trans*-2-hexene in CH_2Cl_2 at 25 °C and 1 atm of N_2 over that of its parent complex, $Ru(H)_2(CO)(PPh_3)_3$.

† On leave from the Universidad de Alcala de Henares, Spain.

(1) Mueting, A. M.; Bos, W.; Alexander, B. D.; Boyle, P. D.; Casalnuovo, J. A.; Balaban, S.; Ito, L. N.; Johnson, S. M.; Pignolet, L. H. Recent Advances in Di- and Polynuclear Chemistry; Braunstein, P., Ed.; *New. J. Chem.* **1988**, *12*, and references cited therein.
(2) Alexander, B. D.; Johnson, B. J.; Johnson, S. M.; Boyle, P. D.; Kann, N. C.; Mueting, A. M.; Pignolet, L. H. *Inorg. Chem.* **1987**, *26*, 3506.
(3) Boyle, P. D.; Johnson, B. J.; Alexander, B. D.; Casalnuovo, J. A.; Gannon, P. R.; Johnson, S. M.; Larka, E. A.; Mueting, A. M.; Pignolet, L. H. *Inorg. Chem.* **1987**, *26*, 1346.
(4) Alexander, B. D.; Boyle, P. D.; Johnson, B. J.; Johnson, S. M.; Casalnuovo, J. A.; Mueting, A. M.; Pignolet, L. H. *Inorg. Chem.* **1987**, *26*, 2547.
(5) Alexander, B. D.; Johnson, B. J.; Johnson, S. M.; Casalnuovo, A. L.; Pignolet L. H. *J. Am. Chem. Soc.* **1986**, *108*, 4409.
(6) Boyle, P. D.; Johnson, B. J.; Buehler, A.; Pignolet, L. H. *Inorg. Chem.* **1986**, *25*, 5.
(7) Casalnuovo, A. L.; Laska, T.; Nilsson, P. V.; Olofson, J.; Pignolet, L. H. *Inorg. Chem.* **1985**, *24*, 233.
(8) Casalnuovo, A. L.; Laska, T.; Nilsson, P. V.; Olofson, J.; Pignolet, L. H.; Bos, W.; Bour, J. J.; Steggarda, J. J. *Inorg. Chem.* **1985**, *24*, 182.
(9) Casalnuovo, A. L.; Casalnuovo, J. A.; Nilsson, P. V.; Pignolet, L. H. *Inorg. Chem.* **1985**, *24*, 2554.
(10) Casalnuovo, A. L.; Pignolet, L. H.; van der Velden, J. W. A.; Bour, J. J.; Steggerda, J. J. *J. Am. Chem. Soc.* **1983**, *105*, 5957.
(11) Bos, W.; Steggerda, J. J.; Shiping, Y.; Casalnuovo, J. A.; Mueting, A. M.; Pignolet, L. H. *Inorg. Chem.* **1988**, *27*, 948.
(12) Bour, J. J.; Kanters, R. P. F.; Schlebos, P. P. J.; Bos, W.; Bosman, W. P.; Behm, H.; Beurskens, P. T.; Steggerda, J. J. *J. Organomet. Chem.* **1987**, *329*, 405.
(13) Jones, P. G. *Gold Bull.* **1986**, *19*, 46 and references cited therein.
(14) Braunstein, P.; Rosé, J. *Gold Bull.* **1985**, *18*, 17.
(15) Hall, K. P.; Mingos, D. M. P. *Prog. Inorg. Chem.* **1984**, *32*, 237 and references cited therein.
(16) Jones, P. G. *Gold Bull.* **1983**, *16*, 114 and references cited therein.
(17) Manojlović-Muir, L.; Muir, K. W.; Treurnicht, I.; Puddephatt, R. J. *Inorg. Chem.* **1987**, *26*, 2418.
(18) Albinati, A.; Lehner, H.; Venanzi, L. M.; Wolfer, M. *Inorg. Chem.* **1987**, *26*, 3933.
(19) Evans, J.; Street, A. C.; Webster, M. *Organometallics* **1987**, *6*, 794.
(20) Freeman, M. J.; Orpen, A. G.; Salter, I. D. *J. Chem. Soc., Dalton Trans.* **1987**, 397, 1001.
(21) Murray, H. H.; Briggs, D. A.; Garzón, G.; Raptis, R. G.; Porter, L. C.; Fackler, J. P., Jr. *Organometallics* **1987**, *6*, 1992.
(22) Blohm, M. L.; Gladfelter, W. L. *Inorg. Chem.* **1987**, *26*, 459.
(23) Housecroft, C. E.; Rheingold, A. L. *Organometallics* **1987**, *6*, 1332.
(24) Blagg, A.; Shaw, B. L.; Thornton-Pett, M. *J. Chem. Soc., Dalton Trans.* **1987**, 769.

0020-1669/88/1327-3301$01.50/0

Experimental Section

Physical Measurements and Reagents. ^1H and ^{31}P NMR spectra were recorded at 300 and 121.5 MHz, respectively, with the use of a Nicolet NT-300 spectrometer. ^{31}P NMR spectra were run with proton decoupling and are reported in ppm relative to internal standard trimethyl phosphate (TMP), with positive shifts downfield. CP MAS ^{31}P NMR spectra were run on an IBM NR100AF spectrometer with a solids' accessory and a DOTY MAS multinuclear probe. Infrared spectra were recorded on a Perkin-Elmer 1710 FT-IR spectrometer. Conductivity measurements were made with use of Yellow Springs Model 31 conductivity bridge. Compound concentrations used in the conductivity experiments were 3×10^{-4} M in CH_3CN. FABMS experiments were carried out with use of a VG Analytical, Ltd., 7070E-HF high-resolution double-focusing mass spectrometer equipped with a VG 11/250 data system.[3] Microanalyses were carried out by M-H-W Laboratories, Phoenix, AZ. Solvents were dried and distilled prior to use. $AuPPh_3NO_3$,[44] $Os(H)_4(PPh_3)_3$,[45] $Os(H)_2(CO)(PPh_3)_3$,[46] $Os(H)_2(CO)_2(PPh_3)_2$,[47] $Ru(H)_4(PPh_3)_3$,[48] $Ru(H)_2(CO)(PPh_3)_3$,[49] and $Ru(H)_2(CO)_2(PPh_3)_2$[50] were prepared as described in the literature. NH_4PF_6 was purchased from Aldrich Chemical Co. All manipulations were carried out under a purified N_2 atmosphere with use of standard Schlenk techniques unless otherwise noted.

Preparation of Compounds. **$[Au_2Os(H)_3(PPh_3)_5]PF_6$ (1)** was prepared by reaction of a CH_2Cl_2 suspension of $Os(H)_4(PPh_3)_3$ (10 mL, 623 mg, 0.635 mmol) with a CH_2Cl_2 solution of $AuPPh_3NO_3$ (10 mL, 662 mg, 1.27 mmol) at 0 °C. The resulting solution was allowed to warm to room temperature and then stirred for 1 h, during which time the osmium complex dissolved and a black solution resulted. Concentration of the solution and precipitation with Et_2O resulted in a dark gray product. The solid was collected and redissolved in a minimum amount of CH_2Cl_2, and the mixture was filtered into a MeOH solution that contained 660 mg of NH_4PF_6, forming a light gray precipitate. This precipitate was collected, washed with MeOH followed by Et_2O, and then redissolved in CH_2Cl_2. Filtration of this solution through diatomaceous earth resulted in a clear pale yellow solution that precipitated a white solid in 60% yield upon the addition of Et_2O. Recrystallization from a CH_2Cl_2/Et_2O solvent mixture at ambient temperature produced clear white crystals suitable for X-ray diffraction. ^{31}P NMR (CD_2Cl_2, −70 °C): δ 48.6 (P_A, br s, int = 2), 21.8 (P_B, br s, int = 1), 5.7 (P_C, s, int = 2). CP MAS ^{31}P NMR (25 °C): δ 56.8 and 48.8 (P_A), 19.6 (P_B, br s), 5.8 (P_C, br s). ^1H NMR in hydride region (CD_2Cl_2, −70 °C): δ −4.1 (H_B, m, $J_{H_B-P_A}$ = 27.3 Hz, $J_{H_B-P_B}$ = 23.4 Hz, $J_{H_B-P_C}$ = 15.4 Hz, int = 1), −5.5 (H_A, d of d of t, $J_{H_A-P_A}$ = 57.6 Hz, $J_{H_A-P_B}$ = 15.9 Hz, $J_{H_A-P_C}$ = 7.8 Hz, int = 2). Equivalent conductance (87.1 cm^2 mhos mol^{-1}) is indicative of a 1:1 electrolyte in CH_3CN solution. FABMS (*m*-nitrobenzyl alcohol matrix): *m/z* 1899 ($((Au_2Os(H)_3(PPh_3)_5)^+ = (M)^+$), 1633 ($(M - 3H - PPh_3)^+$), 1557 ($(M - 2H - PPh_3 - Ph)^+$). Anal. Calcd for $Au_2OsP_6C_{90}H_{78}F_6$: C, 52.90; H, 3.85; P, 9.09. Found: C, 53.31; H, 3.99; P, 8.89.

$[Au_2Ru(H)_3(PPh_3)_5]PF_6$ (2) was prepared by reaction of a toluene suspension of $Ru(H)_4(PPh_3)_3$ (15 mL, 349 mg, 0.392 mmol) with a toluene solution of $AuPPh_3NO_3$ (15 mL, 450 mg, 0.863 mmol) under 1 atm of H_2 at ambient temperature. An immediate reaction took place that led to complete dissolution of the ruthenium complex followed by the precipitation of a pale yellow product. The suspension was placed under a N_2 atmosphere and allowed to stir for 1 h. The solid was collected, washed with toluene, and redissolved in a minimum amount of CH_2Cl_2, and the mixture was filtered into a MeOH solution containing 385 mg of NH_4PF_6. An off-white precipitate formed, which was collected and washed with MeOH followed by Et_2O (40% yield). ^{31}P NMR (CD_2Cl_2, 25 °C): δ 56.3 (P_B, m, int = 1), 46.7 (P_C, d, J = 24.0 Hz, int = 2), 43.3 (P_A, d, int = 2). ^1H NMR in hydride region (CD_2Cl_2, −70 °C): δ −3.5 (H_B, br m, int = 1), −4.2 (H_A, br d of m, $J_{H_A-P_A}$ = 67.2 Hz, int = 2). Equivalent conductance (CH_3CN): 84.6 cm^2 mhos mol^{-1}. FABMS (*m*-nitrobenzyl alcohol matrix): *m/z* 1809 ($((Au_2Ru(H)_3(PPh_3)_5)^+ = (M)^+$), 1545 ($(M - 2H - PPh_3)^+$). Anal. Calcd for $Au_2RuP_6C_{90}H_{78}F_6$: C, 55.31; H, 4.02; P, 9.51. Found: C, 55.85; H, 4.29; P, 8.76.

$[AuRu(H)_2(CO)(PPh_3)_4]PF_6$ (3) was prepared by reaction of a CH_2Cl_2 suspension of $Ru(H)_2(CO)(PPh_3)_3$ (5 mL, 530 mg, 0.577 mmol) with a CH_2Cl_2 solution of $AuPPh_3NO_3$ (7 mL, 316 mg, 0.607 mmol) at −30 °C. The solution was warmed to 0 °C and then stirred for 1 h, during which time the ruthenium complex dissolved and a very pale yellow solution resulted. Concentration of the solution and precipitation with Et_2O resulted in an off-white product. The solid was collected and redissolved in a minimal amount of cold CH_2Cl_2, and the mixture was filtered into a MeOH solution that contained 710 mg of NH_4PF_6. The solution was cooled to −70 °C, at which time a white precipitate formed. The product was collected, washed with cold MeOH, toluene, and Et_2O, and then redissolved in cold CH_2Cl_2. Filtration of this solution through diatomaceous earth resulted in a clear pale yellow solution. Upon cooling of this solution to −30 °C and addition of Et_2O, a white solid precipitated in 79% yield. Recrystallization from a CH_2Cl_2/hexane solvent mixture at ambient temperature produced clear white crystals suitable for X-ray diffraction. ^{31}P NMR (acetone-d_6, 25 °C): δ 41.8 (P_A, d, J = 20.1 Hz, int = 1), 41.0 (P_C, q, J = 20.4 Hz, int = 1), 37.2 (P_B, d, J = 20.8 Hz, int = 2). ^1H NMR in hydride region (acetone-d_6, 25 °C): δ −2.7 (H_A, d of quint, $J_{H_A-P_A}$ = 70.9 Hz, int = 1), −5.4 (H_B, m, int = 1). IR (Nujol): ν(CO) 1954 cm^{-1}. Equivalent conductance (CH_3CN): 84.3 cm^2 mhos mol^{-1}. FABMS (*m*-nitrobenzyl alcohol matrix): *m/z* 1377 ($((AuRu(H)_2(CO)(PPh_3)_4)^+ = (M)^+$), 1113 ($(M - 2H - PPh_3)^+$). Anal. Calcd for $AuRuP_5C_{73}H_{62}OF_6$: C, 57.59; H, 4.13; P, 10.17. Found: C, 56.90; H, 4.38; P, 9.47.

$[AuOs(H)_2(CO)(PPh_3)_4]PF_6$ (4) was prepared by reaction of a CH_2Cl_2 suspension of $Os(H)_2(CO)(PPh_3)_3$ (5 mL, 490 mg, 0.487 mmol) with a CH_2Cl_2 solution of $AuPPh_3NO_3$ (5 mL, 256 mg, 0.492 mmol) at ambient temperature. A clear solution resulted that gradually turned pale yellow after stirring for 1 h. Concentration of this solution and precipitation with Et_2O resulted in a white product. The solid was collected, redissolved in a minimum amount of CH_2Cl_2, and the mixture was filtered into a MeOH solution that contained 600 mg of NH_4PF_6. A grayish white precipitate formed, which was collected, washed with MeOH followed by Et_2O, and then redissolved in CH_2Cl_2. Filtration of this solution through diatomaceous earth resulted in a clear pale yellow solution that precipitated a white solid in 60% yield upon the addition of Et_2O. ^{31}P NMR (acetone-d_6, 25 °C): δ 46.4 (P_A, d, $J_{P_A-P_C}$ = 23.5 Hz, int = 1), 10.2 (P_C, d of t, $J_{P_A-P_C}$ = 23.5 Hz, $J_{P_B-P_C}$ = 14.9 Hz, int = 1), −0.7 (P_B, d, $J_{P_B-P_C}$ = 14.9 Hz, int = 2). ^1H NMR in hydride region (acetone-d_6, 25 °C): δ −3.4 (H_A, d of quint, $J_{H_A-P_A}$ = 59.8 Hz, $J_{H_A-P_B}$ = 7.3 Hz, $J_{H_A-P_C}$ = 13.8 Hz, $J_{H_A-H_B}$ = 3 Hz, int = 1), −6.2 (H_B, m, $J_{H_B-P_A}$ = 28.2 Hz, $J_{H_B-P_B}$ = 17.5 Hz, $J_{H_B-P_C}$ = 34.0 Hz, $J_{H_A-H_B}$ = 3 Hz, int = 1). IR (Nujol): ν(CO) 1946 cm^{-1}. Equivalent conductance: 87.8 cm^2 mhos mol^{-1}). FABMS (*m*-nitrobenzyl alcohol matrix): *m/z* 1467 ($((AuOs(H)_2(CO)(PPh_3)_4)^+ = (M)^+$), 1203 ($(M - 2H - PPh_3)^+$). Anal. Calcd for $AuOsP_5C_{73}H_{62}F_6O$: C, 54.42; H, 3.88; P, 9.61. Found: C, 54.40; H, 4.01; P, 9.92.

(25) Green, M.; Howard, J. A. K.; James, A. P.; Nunn, C. M.; Stone, F. G. A. *J. Chem. Soc., Dalton Trans.* **1987**, 61.
(26) Brown, S. S. D.; Salter, I. D.; Adatia, T.; McPartlin, M. *J. Organomet. Chem.* **1987**, *332*, C6.
(27) Low, A. A.; Lauher, J. W. *Inorg. Chem.* **1987**, *26*, 3863.
(28) Horton, A. D.; Mays, M. J.; McPartlin, M. *J. Chem. Soc., Chem. Commun.* **1987**, 424.
(29) Mingos, D. M. P.; Oster, P.; Sherman, D. J. *J. Organomet. Chem.* **1987**, *320*, 257.
(30) Bruce, M. I.; Williams, M. L.; Patrick, J. M.; Skelton, B. W.; White, A. H. *J. Chem. Soc., Dalton Trans.* **1986**, 2557.
(31) Johnson, B. F. G.; Lewis, J.; Nelson, W. J. H.; Vargas, M. D.; Braga, D.; Henrick, K.; McPartlin, M. *J. Chem. Soc., Dalton Trans.* **1986**, 975.
(32) Drake, S. R.; Henrick, K.; Johnson, B. F. G.; Lewis, J.; McPartlin, M.; Morris, J. *J. Chem. Soc., Chem. Commun.* **1986**, 928.
(33) Deeming, A. J.; Donovan-Mtunzi, S.; Hardcastle, K. *J. Chem. Soc., Dalton Trans.* **1986**, 543.
(34) Puga, J.; Sánchez-Delgado, R. A.; Ascanio, J.; Braga, D. *J. Chem. Soc., Chem. Commun.* **1986**, 1631.
(35) Farrugia, L. J. *Acta Crystallogr., Sect. C: Cryst. Struct. Commun.* **1986**, *C42*, 680.
(36) Bos, W.; Bour, J. J.; Schlebos, P. P. J.; Hageman, P.; Bosman, W. P.; Smits, J. M. M.; van Weitmarschen, J. A. C.; Beurskens, P. T. *Inorg. Chim. Acta* **1986**, *119*, 141.
(37) Sinfelt, J. H. *Bimetallic Catalysts*; Wiley: New York, 1983; Chapters 1 and 2.
(38) Evans, J.; Jingxing, G. *J. Chem. Soc., Chem. Commun.* **1985**, 39.
(39) Schwank, J.; Outka, D. A.; Madix, R. J. Papers presented at the ACS Symposium on Catalysis of the Group 1B Metals, 189th National Meeting of the American Chemical Society, Miami Beach, FL, May 1–2, 1985.
(40) Schwank, J. *Gold Bull.* **1985**, *18*, 2; **1983**, *16*, 103.
(41) Wachs, I. E. *Gold Bull.* **1983**, *16*, 98.
(42) Exxon Research and Engineering Co., Eur. Patent 37700; U.S. Patent 4301086, U.S. Patent 4342838.
(43) Union Carbide Corp., U.S. Patent 3878292.
(44) Malatesta, J.; Naldini, L.; Simonetta, G.; Cariati, F. *Coord. Chem. Rev.* **1966**, *1*, 255.
(45) Ahmad, N.; Levison, J. J.; Robinson, S. D.; Uttley, M. F. *Inorg. Synth.* **1974**, *15*, 56.
(46) Ahmad, N.; Levison, J. J.; Robinson, S. D.; Uttley, M. F. *Inorg. Synth.* **1974**, *15*, 54.
(47) Ahmad, N.; Levison, J. J.; Robinson, S. D.; Uttley, M. F. *Inorg. Synth.* **1974**, *15*, 55.
(48) Harris, R. O.; Hota, N. K.; Sadavoy, L.; Yuen, J. M. C. *J. Organomet. Chem.* **1973**, *54*, 259.
(49) Ahmad, N.; Levison, J. J.; Robinson, S. D.; Uttley, M. F. *Inorg. Synth.* **1974**, *15*, 48.
(50) Cenini, S.; Ponta, F.; Pizzotti, M. *Inorg. Chim. Acta* **1976**, *20*, 119.

Table I. Crystallographic Data for **1** and **3**

	$[Au_2Os(H)_3(PPh_3)_5]PF_6 \cdot 3CH_2Cl_2 \cdot 2Et_2O$ (**1**·$3CH_2Cl_2$·$2Et_2O$)	$[AuRu(H)_2(CO)(PPh_3)_4]PF_6 \cdot 2CH_2Cl_2$ (**3**·$2CH_2Cl_2$)
Crystal Parameters and Measurement of Intensity Data		
space group	$P2_1/n$	$P\bar{1}$
T, °C	−116	22
cell params		
a, Å	13.64 (2)	15.404 (3)
b, Å	40.89 (2)	19.461 (8)
c, Å	17.53 (1)	13.868 (7)
α, deg	90	98.86 (4)
β, deg	102.54 (9)	105.68 (3)
γ, deg	90	87.73 (2)
V, Å^3	9550 (20)	3955 (5)
Z	4	2
calcd density, g cm^{-3}	1.702	1.42
abs coeff, cm^{-1}	47.2	22.4
max, min, av trans factors	1.00, 0.82, 0.93	1.00, 0.86, 0.94
formula	$C_{101}H_{104}Cl_6F_6O_2P_6Au_2Os$	$C_{75}H_{66}Cl_4F_6OP_5AuRu$
fw	2446.62	1692.02
radiation	Mo Kα (λ = 0.71069 Å) graphite monochromatized	
Refinement by Full-Matrix Least Squares		
R^a	0.051	0.051
$R_w{}^a$	0.069	0.063

[a] The function minimized was $\sum w(|F_o| - |F_c|)^2$, where $w = 1/[\sigma(F_o)]^2$. The unweighted and weighted residuals are defined as $R = \sum(||F_o| - |F_c||)/\sum|F_o|$ and $R_w = [(\sum w(|F_o| - |F_c|)^2)/(\sum w|F_o|^2)]^{1/2}$. The error in an observation of unit weight (GOF) is $[\sum w(|F_o| - |F_c|)^2/(NO - NV)]^{1/2}$, where NO and NV are the number of observations and variables, respectively.

$[AuOs(H)_2(CO)_2(PPh_3)_3]PF_6$ (5) was prepared by the reaction of $Os(H)_2(CO)_2(PPh_3)_2$ (313 mg, 0.41 mmol) with $AuPPh_3NO_3$ (233 mg, 0.45 mmol) in 5 mL of CH_2Cl_2. The resulting grayish brown solution was stirred for 1 h. Concentration of the solution and precipitation with Et_2O resulted in a dark gray product. The solid was collected and redissolved in a minimum amount of CH_2Cl_2, and the mixture was filtered into a MeOH solution containing 260 mg of NH_4PF_6. A light gray precipitate formed, which was collected, washed with MeOH followed by Et_2O, and then redissolved in CH_2Cl_2. Filtration of this solution through diatomaceous earth resulted in a clear pale yellow solution that precipitated a white solid in 53% yield upon the addition of Et_2O. ^{31}P NMR (acetone-d_6, 25 °C): δ 46.4 (P_A, s, int = 1), 1.3 (P_B, s, int = 2). ^1H NMR in hydride region (acetone-d_6, 25 °C): δ −3.6 (d of t, J_{H-P_A} = 45.8 Hz, J_{H-P_B} = 12.2 Hz, int = 2). IR (Nujol): ν(CO) 2033, 1982 cm^{-1}. Equivalent conductance: 81.2 cm^2 mhos mol^{-1}). FABMS (*m*-nitrobenzyl alcohol matrix): m/z 1233 ($(AuOs(H)_2(CO)_2(PPh_3)_3)^+ = (M)^+$) overlapped with peak at m/z 1231 due to loss of two H atoms. Anal. Calcd for $AuOsP_4C_{56}H_{47}F_6O_2$: C, 48.85; H, 3.44; P, 8.99. Found: C, 49.05; H, 3.74; P, 9.25.

$[AuRu(H)_2(CO)_2(PPh_3)_3]PF_6$ (6) was prepared by reaction of a CH_2Cl_2 suspension of $Ru(H)_2(CO)_2(PPh_3)_2$ (7 mL, 246 mg, 0.360 mmol) with a CH_2Cl_2 solution of $AuPPh_3NO_3$ (5 mL, 192 mg, 0.368 mmol) at 0 °C. The solution was stirred for 1.5 h at 0 °C, resulting in a golden yellow solution. Concentration of the solution and precipitation with Et_2O resulted in an off-white product. The solid was collected, washed with EtOH, and redissolved in a minimum amount of CH_2Cl_2, and the mixture was filtered into a MeOH solution that contained 137 mg of NH_4PF_6. A white precipitate formed, which was collected, washed with MeOH followed by Et_2O, and dried in vacuo (33% yield). ^{31}P NMR (CD_2Cl_2, 25 °C): δ 42.1 (P_A, s, int = 1), 37.3 (P_B, s, int = 2). ^1H NMR in hydride region (CD_2Cl_2, 25 °C): δ −3.3 (d of t, J_{H-P_A} = 50.9 Hz, J_{H-P_B} = 14.7 Hz, int = 2). IR (Nujol): ν(CO) 2059, 2006 cm^{-1}. Equivalent conductance (CH_3CN): 82.2 cm^2 mhos mol^{-1}. FABMS (*m*-nitrobenzyl alcohol matrix): m/z 1143 ($(AuRu(H)_2(CO)_2(PPh_3)_3)^+ = (M)^+$), 1113 ($(M - 2H - CO)^+$). Anal. Calcd for $AuRuP_4C_{56}H_{47}O_2F_6$: C, 52.22; H, 3.68. Found: C, 51.36; H, 3.76.

X-ray Structure Determinations. Collection and Reduction of X-ray Data. A summary of crystal data is presented in Table I. A rectangular crystal of $[Au_2Os(H)_3(PPh_3)_5]PF_6 \cdot 3CH_2Cl_2 \cdot 2Et_2O$ (**1**·$3CH_2Cl_2$·$2Et_2O$) was coated with a viscous high-molecular-weight hydrocarbon and secured on a glass fiber by cooling to −116 °C. A rectangular crystal of $[AuRu(H)_2(CO)(PPh_3)_4]PF_6 \cdot 2CH_2Cl_2$ (**3**·$2CH_2Cl_2$) was sealed inside a capillary tube filled with dichloromethane/hexane solution, since the crystal was found to slowly lose solvent. The crystal classes and space groups were unambiguously determined by the Enraf-Nonius CAD4-SDP-PLUS peak search, centering, and indexing programs,[51] from the systematic absences observed during data collection, and by successful solution and refinement of the structures (vide infra). The intensities of three standard reflections were measured every 1.5 h of X-ray exposure time during data collection, and no decay was observed for **1**. The decay for **3** was linear with a total decrease of 7% and was corrected for with the SDP program DECAY using maximum and minimum correction factors of 1.04 and 1.00.[51] The data were corrected for Lorentz, polarization, and background effects. Empirical absorption corrections were applied for both compounds by use of ψ-scan data and the program EAC.[51]

Table II. Positional Parameters and Their Estimated Standard Deviations for Core Atoms in $[Au_2Os(H)_3(PPh_3)_5]PF_6 \cdot 3CH_2Cl_2 \cdot 2Et_2O$ (**1**·$3CH_2Cl_2$·$2Et_2O$)[a]

atom	x	y	z	B, Å^2
Au1	−0.14439 (3)	0.18374 (1)	0.22376 (3)	1.426 (8)
Au2	−0.22884 (3)	0.10870 (1)	0.05201 (3)	1.464 (8)
Os	−0.11303 (3)	0.16248 (1)	0.08465 (3)	1.039 (8)
P1	−0.1854 (2)	0.19742 (8)	0.3373 (2)	1.37 (6)
P2	−0.3311 (2)	0.06476 (7)	0.0392 (2)	1.60 (6)
P3	0.0093 (2)	0.12885 (7)	0.1633 (2)	1.34 (6)
P4	−0.2513 (2)	0.19726 (7)	0.0339 (2)	1.20 (5)
P5	0.0002 (2)	0.18506 (7)	0.0124 (2)	1.20 (5)

[a] Counterion, solvent molecule, and phenyl group positional parameters are provided in the supplementary material. Anisotropically refined atoms are given in the form of the isotropic equivalent thermal parameter defined as $(4/3)[a^2\beta(1,1) + b^2\beta(2,2) + c^2\beta(3,3) + ab(\cos\gamma)\beta(1,2) + ac(\cos\beta)\beta(1,3) + bc(\cos\alpha)\beta(2,3)]$.

Solution and Refinement of the Structures. The structures were solved by conventional heavy-atom techniques. The metal atoms were located by Patterson syntheses. Full-matrix least-squares refinement and difference Fourier calculations were used to locate all remaining non-hydrogen atoms. The atomic scattering factors were taken from the usual tabulation,[52] and the effects of anomalous dispersion were included in F_c by using Cromer and Ibers' values of $\Delta f'$ and $\Delta f''$.[53] Corrections for extinction were applied. Most non-hydrogen atoms in both **1** and **3** were refined with anisotropic thermal parameters; however, for compound **1** the phenyl ring carbon atoms, C5B and C2J, and one of the diethyl ether molecules were refined isotropically because the temperature factors for these atoms were not well-behaved during refinement. This was also true for the chlorine atoms in the solvate molecules of **3**. The carbon atoms in the solvate molecules of **3** were not located in the difference Fourier maps. This disordered behavior of solvate molecules in large cluster compounds is quite common and generally has little effect on the structure of the cluster. The positions of the hydrogen atoms in the PPh_3 ligands were calculated for **3** and included in the structure factor calculations but were not refined. Only one metal hydride showed up in the final difference Fourier map of **3** and was successfully included in the refinement. In **1** the final difference Fourier map showed reasonable positions for the metal hydrides; however, they did not refine in a convincing manner so were not included in the final stages of refinement. Difference Fourier maps based on low-angle data were calculated for **1**, but this did not enhance the heights of the peaks seen in the difference maps that were suspected to be due to the hydride ligands. The largest peak in the final difference Fourier map of **1** was ca. 2.8 e Å^{-3} and was located near the disordered ether. The largest peak in **3** was ca. 1.08 e Å^{-3} and was located near one of the dichloromethane solvate molecules. The final positional and thermal parameters of the refined atoms within the coordination cores are given in Tables II and III. ORTEP drawings of the cations including the labeling schemes and selected distances and angles are shown in Figures 1 and 4. Complete listings of thermal parameters, positional parameters, calculated positions for the hydrogen atoms, distances, angles, least-squares planes, and structure factor amplitudes are included as supplementary material.[54]

(51) All calculations were carried out on PDP 8A and 11/34 computers with use of the Enraf-Nonius CAD4-SDP programs. This crystallographic computing package is described by: Frenz, B. A. in *Computing in Crystallography*; Schenk, H., Olthoff-Hazekamp, R., van Koningsveld, H., Bassi, G. C., Eds.; Delft University Press: Delft, Holland, 1978; pp 64–71. *CAD 4 User's Manual*; Enraf-Nonius: Delft, Holland, 1978.

(52) Cromer, D. T.; Waber, J. T. In *International Tables for X-Ray Crystallography*; Kynoch: Birmingham, England, 1974; Vol. IV, Table 2.2.4.

(53) Cromer, D. T. In *International Tables for X-Ray Crystallography*; Kynoch: Birmingham, England, 1974; Vol. IV, Table 2.3.1.

(54) See paragraph at end of paper regarding supplementary material.

Table III. Positional Parameters and Their Estimated Standard Deviations for Core Atoms in $[AuRu(H)_2(CO)(PPh_3)_4]PF_6 \cdot 2CH_2Cl_2$ ($3 \cdot 2CH_2Cl_2$)[a]

atom	x	y	z	B, Å^2
Au	−0.30167 (2)	−0.20657 (2)	0.00534 (2)	3.770 (6)
Ru	−0.22809 (4)	−0.13899 (3)	0.20115 (4)	2.70 (1)
P1	−0.3304 (2)	−0.2844 (1)	−0.1401 (2)	3.81 (5)
P2	−0.3140 (1)	−0.0443 (1)	0.2702 (1)	2.99 (4)
P3	−0.1381 (1)	−0.0774 (1)	0.1296 (1)	2.91 (4)
P4	−0.2787 (2)	−0.2378 (1)	0.2579 (2)	3.44 (4)
H	−0.320 (3)	−0.145 (3)	0.090 (4)	1 (1)*
C	−0.1261 (5)	−0.1413 (4)	0.3095 (6)	3.6 (2)
O	−0.0596 (4)	−0.1456 (3)	0.3728 (5)	5.5 (2)

[a] Counterion, solvent molecule, and phenyl group positional parameters are provided in the supplementary material. The asterisk indicates that the atom was refined isotropically. Anisotropically refined atoms are given in the form of the isotropic equivalent thermal parameter defined as $(4/3)[a^2\beta(1,1) + b^2\beta(2,2) + c^2\beta(3,3) + ab(\cos\gamma)\beta(1,2) + ac(\cos\beta)\beta(1,3) + bc(\cos\alpha)\beta(2,3)]$.

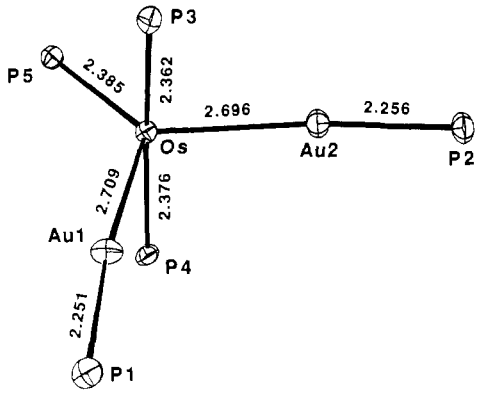

Figure 1. ORTEP drawing of the coordination core of the cation of **1** with selected bond distance (Å). Ellipsoids are drawn with 50% probability boundaries. Phenyl rings have been omitted for clarity. Selected angles (deg) are as follows: Os–Au1–P1, 173.46 (6); Os–Au2–P2, 172.81 (6); Au1–Os–Au2, 104.66 (1); Au1–Os–P3; 83.75 (5); Au1–Os–P4, 82.96 (5); Au1–Os–P5, 126.91 (5); Au2–Os–P3, 87.48 (5); Au2–Os–P4, 91.60 (5); Au2–Os–P5, 128.33 (5); P3–Os–P4, 165.99 (8); P3–Os–P5, 94.49 (7); P4–Os–P5, 97.02 (7). Average esd's for Au–Os, Au–P, and Os–P distances are 0.001, 0.002, and 0.002 Å, respectively.

Results and Discussion

$[Au_2Os(H)_3(PPh_3)_5]PF_6$ (1). The addition of 2 equiv of $AuPPh_3NO_3$ to $Os(H)_4(PPh_3)_3$ in a CH_2Cl_2 solution produced this cationic gold–osmium compound as the nitrate salt. This product was then metathesized with NH_4PF_6 to give **1** in good yield. A single-crystal X-ray diffraction analysis of this compound was carried out in order to determine the nature of the gold–osmium interactions and the overall structure of the complex. These questions could not be answered from the solution NMR and IR data alone (vide infra).

The structure of the coordination core of the cation of **1** with selected distances and angles is shown in Figure 1. The structure consists of two $Au(PPh_3)$ units bonded to an $Os(PPh_3)_3$ unit forming a somewhat distorted trigonal-bipyramidal geometry. There is an approximately planar $P5Os(AuP)_2$ arrangement and a nearly linear P3–Os–P4 (165.99 (8)°) grouping perpendicular to this plane. The Au–PPh_3 vectors are approximately trans to the osmium atom (Os–Au1–P1 = 173.46 (6)°, Os–Au2–P2 = 172.81 (6)°), which is a general trend seen in complexes of this type.[2,5-10] The Au–Os distances are slightly different (2.696 (1), 2.709 (1) Å) and are within the range of values observed in osmium–gold clusters containing primarily carbonyl ligands [for example, average 2.657 (1) Å in $Os(CO)_4(AuPPh_3)_2$[55] and 2.771 (1) Å in $Os_5C(CO)_{14}(\mu\text{-}AuPPh_3)_2$[56]]. The average Au–P and Os–P distances (2.254 (2) and 2.374 (2) Å, respectively) are within the ranges of values observed in other heterometallic clusters[1,2,5-10] and osmium–phosphine complexes (range 2.29–2.46 Å).[57-59] An unusual aspect of the molecular structure of **1**, when compared to that of the transition-metal–gold complexes containing primarily phosphine ligands,[1] is that there is no Au–Au bond (4.28 Å). The lack of a Au–Au bond is also seen in large osmium carbonyl clusters containing several gold atoms, such as $Os_8(CO)_{22}(\mu\text{-}AuPPh_3)_2$ (4.534 (1) Å).[60] This cluster complex contains gold atoms that bridge Os–Os bonds. In clusters such as this, however, each gold atom is bonded to well-separated sites on the osmium framework rather than both gold atoms bonded to just one osmium site as in complex **1**.

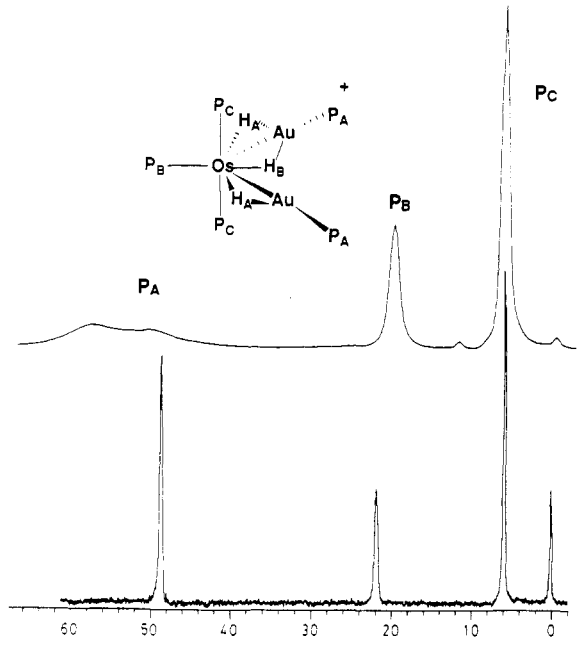

Figure 2. ^{31}P NMR spectra of $[Au_2Os(H)_3(PPh_3)_5]PF_6$ (**1**) in the solid state at 25 °C and in solution at −70 °C. The bottom trace is the $^{31}P\{^1H\}$ NMR spectrum recorded with CH_2Cl_2 as solvent (internal standard trimethyl phosphate, $\delta = 0$), while the upper trace is the CP MAS ^{31}P NMR spectrum.

The absence of a Au–Au bond may be due to the presence of a hydride ligand bridging one of the Au–Os bonds and positioned between the two gold atoms in the Au_2Os plane. The remaining two hydrides are believed to bridge each of the Au–Os bonds approximately in the Au_2Os plane and on the outside edges of the Au_2Os triangle. This arrangement is shown below and in Figures 2 and 3. It appears that the stability of **1** is enhanced by maximization of gold–hydride interactions rather than by formation of a Au–Au bond. In an attempt to locate the hydride positions in the X-ray structure determination, a final difference Fourier map was calculated that gave reasonable positions for the three hydride ligands as described above. When lower values of $(\sin\theta)/\lambda$ were used in the calculation of the difference Fourier map,[61] there was no significant improvement in the height of these peaks over those due to noise and attempts at least-squares refinement were unsuccessful. Although these positions could not be reliably assigned to the hydride ligands, the general positions did seem reasonable when compared to the spectroscopic results.

The ^{31}P NMR solution spectrum of **1** (−70 °C, CD_2Cl_2) is in agreement with its solid-state structure. A trace of the spectrum

(55) Johnson, B. F. G.; Lewis, J.; Raithby, P. R.; Sanders, A. *J. Organomet. Chem.* **1984**, *260*, C29.
(56) Johnson, B. F. G.; Lewis, J.; Nicholls, J. N.; Nelson, W. J. H.; Puga, J.; Vargas, M. D. *J. Chem. Soc., Dalton Trans.* **1983**, 2447.
(57) Bohle, D. S.; Jones, T. C.; Richard, C. E. F.; Roper, W. R. *Organometallics* **1986** *5*, 1612.
(58) Bruno, J. W.; Huffman, J. C.; Caulton, K. G. *J. Am. Chem. Soc.* **1984**, *106*, 1663.
(59) Frost, P. W.; Howard, J. A. K.; Spencer, J. L. *J. Chem. Soc., Chem. Commun.* **1984**, 1362.
(60) Johnson, B. F. G.; Lewis, J.; Nelson, W. J. H.; Raithby, P. R.; Vargas, M. D. *J. Chem. Soc., Chem. Commun.* **1983**, 608.
(61) La Place, S. J.; Ibers, J. A. *Acta Crystallogr.* **1965**, *18*, 511.

is shown in Figure 2 along with that of the CP MAS ^{31}P spectrum of the solid compound. The solution spectrum consists of three singlet resonances (δ 48.6, 21.8, and 5.7) with an intensity ratio of 2:1:2. These resonances are due to the gold phosphines (P_A) and the osmium phosphines (P_B and P_C), respectively. This peak assignment was verified by the synthesis of compound **1** with PMe_2Ph in place of PPh_3 on the gold atom.[62] In this case the only resonance to shift significantly was P_A, from δ 48.6 to δ 21.4 in $[Au_2Os(H)_3(PPh_3)_3(PMe_2Ph)_2]PF_6$. Therefore, the peaks at δ 21.8 and 5.7 are due to the osmium phosphines P_B and P_C, respectively, which shifted only slightly to δ 23.0 and 4.5 in the PMe_2Ph analogue. The solution spectrum of **1** taken at −70 °C is identical with that taken at room temperature, with only slight chemical shift differences. NMR experiments at temperatures below −70 °C were unsuccessful due to solubility problems; however, the solid-state NMR spectrum provided further insight into the molecular structure. The CP MAS ^{31}P spectrum recorded at 25 °C displays two single broad $Au(PPh_3)$ resonances. This is consistent with H_B being locked into one of the two bridging positions, giving two nonequivalent gold phosphines (vide infra). Although solid-state effects may also lead to different resonances for "equivalent" phosphines, the fact that only one of the CP MAS ^{31}P NMR signals was split (see Figure 2) lends support to this conclusion. Also, the nonequivalence of the $Au(PPh_3)$ groups has been directly observed in solution for the ruthenium analogue of this compound by ^{31}P NMR at ca. −130 °C (vide infra).

Infrared analysis of this complex in the solid state (Nujol) showed no absorptions that could be attributed to terminal hydride ligands. Calculation of the optimum hydride positions in **1** with use of Orpen's potential energy minimization computer program[63] predicted bridging hydride positions on the outer edges of the Au–Os bonds.[1] There were three possible positions predicted for the third hydride located between the two gold atoms; however, the lowest potential energy occurred for a Au_2Os triangular face bridging hydride. This result is questionable in light of the solid-state ^{31}P NMR data and the fact that this would result in very long Au–H bonds (ca. 2.2 Å).[1]

The ^1H NMR spectrum of **1** (−70 °C, CD_2Cl_2) was recorded in the hydride region and is shown in Figure 3. The spectrum consists of two multiplet resonances (δ −4.1 and −5.5) with an intensity ratio of 1:2. The selective phosphorus decoupling results support the above assignment of P_A, P_B, and P_C and yielded all of the P–H coupling constants (see Experimental Section and Figure 3). The two multiplets were successfully simulated and are also shown in Figure 3. An important result of this NMR analysis was the determination of the $J(\mu\text{-H–P}_A)$ coupling constant for the three bridging hydrides in the μ-$HAuPPh_3$ unit. The two equivalent hydrides, H_A, gave a $J(\mu\text{-H–P}_A)$ coupling constant of 57.6 Hz.[1,2,5] This value is larger than expected for the structure observed in the solid state, which has a cisoid μ-H–Au–P arrangement. It is smaller, however, than the values of 105 Hz in $[AuCr(\mu\text{-H})(CO)_5(PPh_3)]$,[64] 79.8 Hz in $[(H)_2(PPh_3)_3Ir(\mu\text{-H})AuPPh_3]BF_4$,[65] and 82 Hz in $[AuPt(\mu\text{-H})(C_6F_5)(PEt_3)_2(PPh_3)](CF_3SO_3)$,[18] all of which resulted from a transoid H–Au–PPh_3 arrangement. The magnitude of the μ-*H*Au*P*Ph_3 coupling constant suggests that in solution P_A is not simply trans to the Au–Os bond but is in rapid equilibrium between trans and cis μ-H–Au–P stereochemistries, giving an average and thus larger coupling constant than would be expected due to the stereochemistry seen in the solid-state structure of **1**. The $J(\mu\text{-H–P}_A)$ coupling constant for H_B has a value of 27.3 Hz, approximately half that of H_A. This could be due to an equilibrium process that causes H_B to bridge one of the Au–Os bonds and then the other,

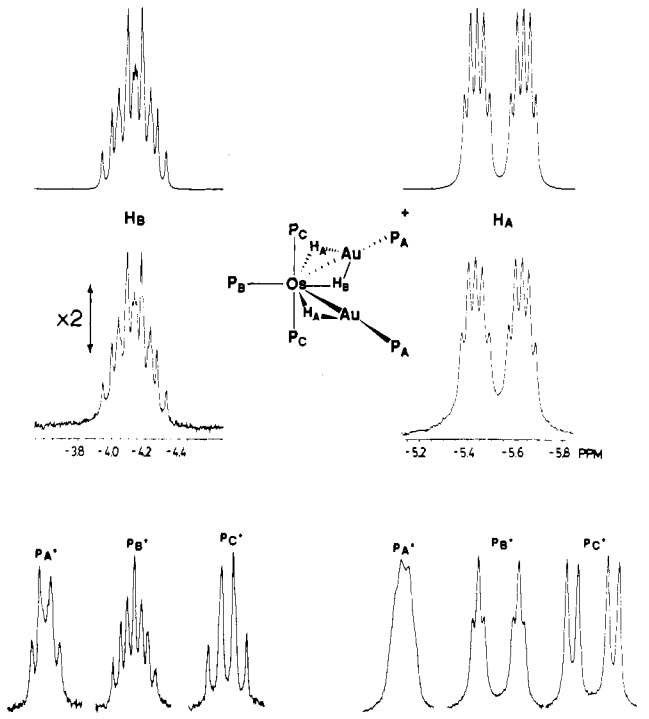

Figure 3. ^1H NMR spectra of $[Au_2Os(H)_3(PPh_3)_5]PF_6$ (**1**) in the hydride region recorded with CD_2Cl_2 as solvent at −70 °C. The upper traces are the simulations based on the following coupling constants (Hz): P_A–H_A, 57.6; P_B–H_A, 15.9; P_C–H_A, 7.8; P_A–H_B, 27.3; P_B–H_B, 23.4; P_C–H_B, 15.4. Lower traces: ^1H NMR with selective ^{31}P decoupling. The starred phosphorus atoms were decoupled as shown. See text for further details.

indicated as follows, thus giving an average and smaller coupling constant for $J(\mu\text{-H}_B\text{–P}_A)$.

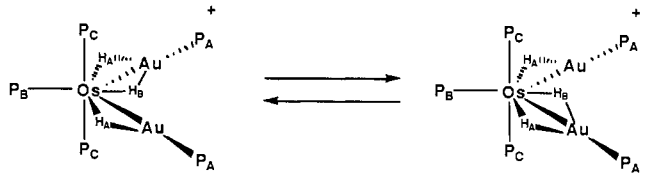

The positive ion FABMS analysis of **1** gives direct evidence for the presence of three hydride ligands. The major highest mass peak at m/z 1899 has an isotopic ion distribution pattern that exactly matches that calculated for the parent cluster ion $[Au_2Os(H)_3(PPh_3)_5]^+$.[3] Equivalent conductance and elemental analysis data provide further support for the formulation of **1** as the 1:1 electrolyte $[Au_2Os(H)_3(PPh_3)_5]PF_6$.

$[Au_2Ru(H)_3(PPh_3)_5]PF_6$ (2), the ruthenium analogue of **1** was synthesized in an analogous manner to that for **1** using $Ru(H)_4(PPh_3)_3$ and ca. 2 equiv of $AuPPh_3NO_3$. The characterization data are all consistent with a structure similar to that of **1**. The ^{31}P NMR solution spectrum (25 °C, CD_2Cl_2) consists of three resonances (δ 56.3, 46.7, and 43.3) with relative intensities of 1:2:2, assigned to the ruthenium phosphines (P_B and P_C) and the gold phosphines (P_A), respectively. These resonances show more fine structure than is seen in the ^{31}P NMR spectrum of **1**; i.e., the peak assigned to the equatorial ruthenium phosphine, P_B, at δ 56.3 appears as a multiplet, and both the axial ruthenium phosphines, P_C, and the gold phosphines, P_A, appear as doublets. These assignments are based on relative integration values and decoupling experiments. Upon decoupling of the resonances at δ 56.3 (P_B) and 46.7 (P_C), the ^1H resonance assigned to H_A collapsed to a broad doublet and that assigned to H_B collapsed slightly but still remained a multiplet in each case. When the ^{31}P resonance at δ 43.3 (H_A) was decoupled, however, the H_A resonance collapsed to a broad singlet and the H_B resonance to a broad doublet. Further verification of the above assignments comes from low-temperature ^{31}P NMR experiments. When the temperature of

(62) This compound was synthesized in a manner analogous to that for **1** except with the use of $Au(PMe_2Ph)NO_3$ in place of $AuPPh_3NO_3$. PMe_2Ph was synthesized according to: Frajerman, C.; Meunier, B. *Inorg. Synth.* **1983**, *22*, 133.
(63) Orpen, A. G. *J. Chem. Soc., Dalton Trans.* **1980**, 2509.
(64) Green, M.; Orpen, A. G.; Salter, I. D.; Stone, F. G. A. *J. Chem. Soc., Dalton Trans.* **1984**, 2497.
(65) Lehner, H.; Matt, D.; Pregosin, P. S.; Venanzi, L. M. *J. Am. Chem. Soc.* **1982**, *104*, 6825.

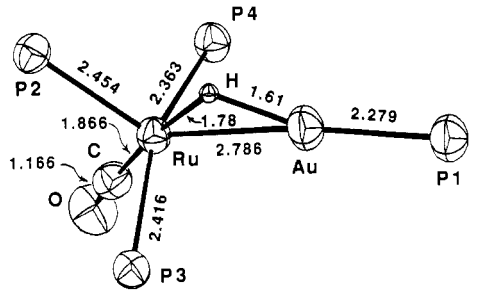

Figure 4. ORTEP drawing of the coordination core of the cation of **3** with selected bond distances (Å). Ellipsoids are drawn with 50% probability boundaries. Phenyl rings have been omitted for clarity. Selected angles (deg) are as follows: Ru–Au–P1, 163.50 (5); Ru–Au–H, 37 (2); P1–Au–H, 159 (2); Au–Ru–H, 33 (1); Au–Ru–P2, 118.39 (4); Au–Ru–P3, 86.25 (4); Au–Ru–P4, 86.36 (4); Au–Ru–C, 140.3 (2); P2–Ru–P3, 101.40 (6); P2–Ru–P4, 101.40 (6); P2–Ru–H, 86 (1); P2–Ru–C, 101.3 (2); P3–Ru–P4, 156.87 (6); P3–Ru–H, 93 (1); P3–Ru–C, 86.3 (2); P4–Ru–H, 93 (1); P4–Ru–C, 85.4 (2); H–Ru–C, 173 (1); Au–H–Ru, 110 (2); Ru–C–O, 175.4 (6). Average esd's for Au–Ru, M–P, Ru–C, C–O, and M–H are 0.001, 0.002, 0.007, 0.008, and 0.04 Å, respectively.

a CH_2Cl_2 solution of **2** was lowered, the doublet at δ 43.3 assigned to P_A broadened and was reduced to a broad singlet. Upon cooling of the sample further to −130 °C (CH_2Cl_2/Freon-12), this resonance shifted slightly and split into two peaks at δ 42.2 and 41.5, providing further support for the nonequivalence of the $Au(PPh_3)$ groups in **2**, as well as its osmium analogue **1**. At this temperature the peaks due to P_B and P_C appeared as broad singlets at δ 55.4 and 47.0, respectively.

The low-temperature ^1H NMR (−70 °C, CD_2Cl_2) spectrum of **2** displays two resonances in the hydride region with an intensity ratio of 1:2. On the basis of analogy to compound **1**, the broad multiplet at δ −3.5 is assigned to the unique hydride H_B, and the broad doublet of multiplets at δ −4.2 is assigned to the two equivalent hydrides H_A, with a $J(\mu\text{-H-}P_A)$ coupling constant of 67.2 Hz. Further support for the formulation of **2** as the 1:1 electrolyte $[Au_2Ru(H)_3(PPh_3)_5]PF_6$ is provided by the equivalent conductance, IR (which showed no evidence for terminal hydrides), FABMS, and elemental analysis data.

$[AuRu(H)_2(CO)(PPh_3)_4]PF_6$ (3). The addition of a slight molar excess of $AuPPh_3NO_3$ to $Ru(H)_2(CO)(PPh_3)_3$ in a CH_2Cl_2 solution at low temperature gave this cationic gold–ruthenium compound as the nitrate salt. This product was then metathesized with NH_4PF_6 to give **3** in good yield. A single-crystal X-ray diffraction analysis of this compound was carried out in order to determine the structure of the complex, since this could not be completely answered from the solution NMR and IR data alone (vide infra).

The structure of the coordination core of the cation of **3** with selected distances and angles is shown in Figure 4. The structure consists of a $Au(PPh_3)$ moiety bonded to a $Ru(CO)(PPh_3)_3$ unit that has a highly distorted trigonal-bipyramidal (TBP) geometry (ignoring the hydride ligands) with $Au(PPh_3)$, P2, and the CO ligands in equatorial positions. The distortion from ideal TBP geometry is manifested by the Au–Ru–CO, Au–Ru–P2, and P2–Ru–CO bond angles of 140.3 (2), 118.39 (4), and 101.3 (2)°, respectively, within the equatorial plane. One of the hydride ligands was located and refined in the crystal structure analysis and is bridging the Au–Ru bond and is trans to the CO ligand (H–Ru–CO = 173 (1)°). There is an approximately planar P2(C)(H)RuAu arrangement with a somewhat linear P3–Ru–P4 (156.87 (6)°) grouping that is perpendicular to this plane and bent slightly toward the open space. Potential energy calculations indicate that the other hydride ligand is occupying this space, bridging the Au–Ru bond and approximately trans to the equatorial Ru–P2 vector.[1] The Au–P1 vector is roughly trans to the ruthenium atom (Ru–Au–P1 = 163.50 (5)°); however, this is not nearly as trans as the Ru–Au–P vectors seen in other complexes (average 172.45 (3) Å in $\{Au_2Ru(H)_2(dppm)_2(PPh_3)_2\}(NO_3)_2$[5] and 170.95 (5) Å in $\{AuRu(H)_2(dppm)_2(PPh_3)\}PF_6$[2]). Furthermore, the Au–P1 vector makes an angle of 159 (2)° with the bridging hydride, H, as compared to an average of 151.0 (2)° in $\{Au_2Ru(H)_2(dppm)_2(PPh_3)_2\}(NO_3)_2$[5] and 141 (2)° in $\{AuRu(H)_2(dppm)_2(PPh_3)\}PF_6$.[2] This hydride bridges somewhat asymmetrically, being closer to the gold atom than to the ruthenium atom (1.61 (4) and 1.78 (4) Å, respectively), but this difference is barely significant considering the large esd's. The Ru–H distance is slightly longer than values previously observed for hydrides bridging Au–Ru bonds (1.61 (4) Å in the $Au_2Ru(dppm)_2$ complex,[5] 1.71 (6) Å in the $AuRu(dppm)_2$ complex,[2] typical range 1.6–1.9 Å[66,67]). The Au–H distance is slightly shorter than previously determined values [1.77 (4) Å in the $Au_2Ru(dppm)_2$ complex,[5] 1.98 (6) Å in the $AuRu(dppm)_2$ complex,[2] 1.7 (1) Å in $AuCr(\mu\text{-H})(CO)_5(PPh_3)$,[64] and 1.72 (9) Å in $[AuPt(\mu\text{-H})(C_6F_5)(PEt_3)_2(PPh_3)](CF_3SO_3)$[18]], but these differences are barely significant. The Au–Ru distance (2.786 (1) Å) is similar to that found in the $Au_2Ru(dppm)_2$ complex (average 2.781 (0) Å)[5] but longer than that in the $AuRu(dppm)_2$ complex (2.694 (1) Å).[2] This result is surprising, since **3** and the $AuRu(dppm)_2$ complex have the same sort of Au–Ru bond bridged by two hydride ligands; however, the shorter Au–Ru bond in the $AuRu(dppm)_2$ complex may be due to the less steric dppm ligands. The Au–P1 distance (2.279 (2) Å) and average Ru–P distances (2.411 (2) Å) compare well to those in the $Au_2Ru(dppm)_2$ complex (2.283 (1) Å and 2.361 (1) Å, respectively)[5] and are similar to values observed in other heterometallic clusters.[1,2,6–10]

The ^{31}P NMR solution spectrum (25 °C, acetone-d_6) of **3** is consistent with its solid-state structure and consists of three peaks (δ 41.8, 41.0, and 37.2) with a relative intensity ratio of 1:1:2. The resonance at δ 41.8 is a doublet and is assigned to the gold phosphine phosphorus (P_A) that is coupled to P_C (J = 20.1 Hz). This peak assignment was verified by synthesis of compound **3** with PMe_2Ph in place of PPh_3 on the gold atom.[68] In this case the only resonance to shift significantly was P_A, δ 13.0 in $[AuRu(H)_2(CO)(PPh_3)_3(PMe_2Ph)]PF_6$. Therefore, the peaks at δ 41.0 and 37.2 are due to the ruthenium phosphines. The P_C atom (δ 41.0) couples to both P_A and the two equivalent P_B atoms, resulting in a pseudoquartet (J = 20.4 Hz), and the P_B atoms (δ 37.2) couple to P_C, resulting in a doublet (J = 20.8 Hz). These peak and coupling constant assignments are further supported by analogy to the assignments made for the osmium analogue **4** (vide infra).

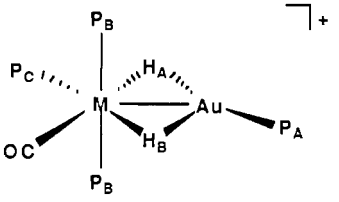

3 (M = Ru) or **4** (M = Os)

The ^1H NMR spectrum of **3** (25 °C, acetone-d_6) was recorded in the hydride region and consists of two multiplet resonances at δ −2.7 and −5.4 (H_A and H_B, respectively). The selective phosphorus decoupling was not done; however, the μ-*H*Au*P*Ph_3 coupling constant $J_{H_A-P_A}$ could be tentatively determined from the spectrum since the peak assigned to H_A at δ −2.7 is a doublet of quintets with a value of 70.9 Hz for the major splitting. Further verification and discussion of this come from a selectively phosphorus-decoupled ^1H NMR experiment and a successful ^{31}P NMR simulation of the osmium analogue **4** (vide infra).

The positive ion FABMS analysis of **3** displays the major highest mass peak at m/z 1377 with an isotopic ion distribution pattern which exactly matches that calculated for the parent cluster ion $[AuRu(H)_2(CO)(PPh_3)_4]^+$.[3] IR analysis (Nujol)

(66) Teller, R. G.; Bau, R. *Struct. Bonding (Berlin)* **1981**, *44*, 1.
(67) Bau, R.; Teller, R. G.; Kirtley, S. W.; Kottzle, T. F. *Acc. Chem. Res.* **1979**, *12*, 176.
(68) This compound was synthesized in a manner analogous to that for **3** except with the use of $Au(PMe_2Ph)NO_3$ in place of $AuPPh_3NO_3$. PMe_2Ph was synthesized according to ref 62.

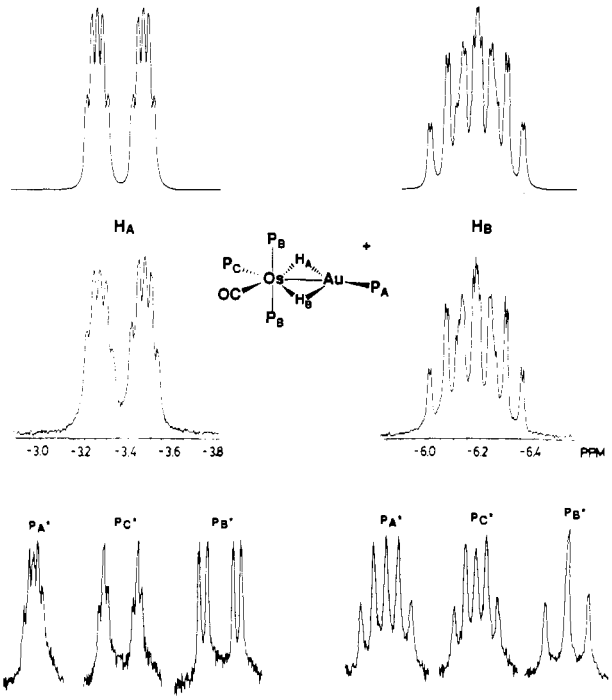

Figure 5. ^1H NMR spectra of $[AuOs(H)_2(CO)(PPh_3)_4]PF_6$ (**4**) in the hydride region recorded with use of acetone-d_6 as solvent at 25 °C. The upper traces are the simulations based on the following coupling constants (Hz): P_A–H_A, 59.8; P_B–H_A, 7.3; P_C–H_A, 13.8; P_A–H_B, 28.23; P_B–H_B, 17.5; P_C–H_B, 34.0; H_A–H_B, 3. Lower traces: ^1H NMR with selective ^{31}P decoupling. The starred phosphorus atoms were decoupled as shown. See text for further details.

displays a CO stretching frequency at 1954 cm^{-1}, a shift of 14 cm^{-1} to higher energy relative to the parent complex, which is consistent with a net positive charge. Equivalent conductance and elemental analysis data provide further evidence for the formulation of **3** as a 1:1 electrolyte.

The reaction of $Os(H)_2(CO)(PPh_3)_3$ with 1 equiv of $AuPPh_3NO_3$ in a CH_2Cl_2 solution followed by metathesis with NH_4PF_6 gave the 1:1 adduct $[AuOs(H)_2(CO)(PPh_3)_4]PF_6$ (**4**) in good yield. The proposed stereochemistry of **4** is analogous to that of **3** and has been deduced from ^{31}P and ^1H NMR and IR spectroscopies.

The ^{31}P NMR spectrum of **4** (25 °C, acetone-d_6) is in agreement with this proposed structure and consists of three resonances (δ 46.4, 10.2, and −0.7) with an intensity ratio of 1:1:2. The doublet at δ 46.4 (P_A) is due to the gold phosphine phosphorus that is coupled to P_C (J = 23.5 Hz) but not to P_B, which would give a small and unobservable coupling to P_A.[2,5] The P_C atom (δ 10.2) couples to P_A and two equivalent P_B atoms, resulting in a doublet of triplets (J = 23.5 Hz, J = 14.9 Hz). The P_B atoms (δ −0.7) couple to P_C, resulting in a doublet (J = 14.9 Hz). A selectively phosphorus-decoupled ^1H NMR experiment (vide infra) and a successful ^{31}P NMR simulation confirmed this AB_2C assignment.

The ^1H NMR spectrum of **4** (25 °C, acetone-d_6) was recorded in the hydride region and is shown in Figure 5 along with its simulated spectrum. The spectrum consists of two multiplet resonances at δ −3.4 and −6.2 (H_A and H_B, respectively). The selective phosphorus decoupling gives the μ-*H*Au*P*Ph$_3$ coupling constant for the two inequivalent hydrides and supports the proposed structure. The stereochemistry proposed should result in a much larger $J(\mu\text{-H–P}_A)$ coupling constant for H_A (59.8 Hz) than for H_B (28.2 Hz), due to the fact that H_A is approximately trans to P_A while H_B is cis. The other coupling constants (see Experimental Section) are also consistent with the proposed structure, as are the IR, conductance, FABMS, and elemental analysis data.

The last two complexes synthesized in this series of osmium– and ruthenium–gold complexes resulted from the reactions of $M(H)_2(CO)_2(PPh_3)_2$ (M = Os, Ru) with 1 equiv of $AuPPh_3NO_3$ in a CH_2Cl_2 solution followed by metathesis with NH_4PF_6. $[AuOs(H)_2(CO)_2(PPh_3)_3]PF_6$ (**5**) was produced at room temperature in good yield, and $[AuRu(H)_2(CO)_2(PPh_3)_3]PF_6$ (**6**) at

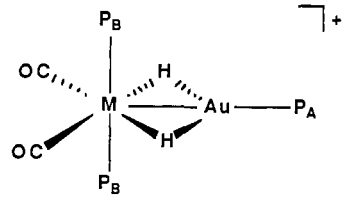

5 (M = Os) or **6** (M = Ru)

0 °C. The formulation of these complexes as 1:1 adducts is based on equivalent conductance, FABMS, and elemental analysis data (see Experimental Section). The proposed trigonal-bipyramidal structures are similar to those of $[AuIr(H)_2(bpy)(PPh_3)_3]BF_4$[5] and $[AuIr(H)_2(PPh_3)_3(NO_3)]BF_4$[8] and are supported by solution NMR and IR analysis.

The ^{31}P NMR spectrum of **5** (25 °C, acetone-d_6) consists of two singlet resonances (δ 46.4 and 1.3) with an intensity ratio of 1:2. These resonances are due to the gold and osmium phosphines (P_A and P_B), respectively. In the ^{31}P NMR spectrum of **6** (25 °C, CD_2Cl_2) the gold phosphine resonance appears at δ 42.1 and the ruthenium phosphine resonance is at δ 37.3. The P_B phosphines are believed to be axial and mutually trans on the basis of the stereochemistry of $M(H)_2(CO)_2(PPh_3)_2$ (M = Os, Ru) and the lack of any observable P_A–P_B coupling. Coupling between a gold phosphine and an equatorial transition-metal phosphine is generally observable and is 20.1 Hz in complex **3**.

The ^1H NMR (25 °C, acetone-d_6) spectrum of **5** consists of a doublet of triplets centered at δ −3.6 with J = 45.8 and 12.2 Hz for the doublet and triplet splittings, respectively. The ^1H NMR (25 °C, CD_2Cl_2) spectrum of **6** consists of a similar pattern centered at δ −3.3 with J = 50.9 and 14.7 Hz. The integration of these hydride signals relative to the phenyl hydrogens indicates the presence of two hydrides in each case. Selective phosphorus decoupling of **5** confirmed that the 45.8-Hz coupling (and, by analogy, the 50.9-Hz coupling observed in **6**) is due to the hydrides coupling to the gold-bound phosphorus atom, P_A. The magnitude of these μ-*H*Au*P*Ph$_3$ coupling constants is intermediate between those of cisoid and transoid μ-H–Au–P geometries and therefore favors a dihydride-bridged arrangement in solution for both **5** and **6** with the gold phosphorus atom in rapid equilibrium between *trans*-M–Au–P and *trans*- and *cis*-μ-H–Au–P stereochemistries.

The positive ion FABMS analyses of **5** and **6** give direct evidence for the presence of two hydride ligands in each complex. The major highest mass peaks at m/z 1233 and 1143, respectively, have an isotopic ion distribution pattern which exactly matches that calculated for the parent cluster ions $[AuM(H)_2(CO)_2(PPh_3)_3]^+$ (M = Os, Ru).[3] Equivalent conductance, IR, and elemental analysis data provide further support for the formulation of **5** and **6** as proposed.

Catalysis. There have been relatively few investigations on the use of transition-metal–gold complexes as homogeneous catalysts. It has been speculated that the addition of a Au(I) fragment to a transition-metal complex may lead to an increase in both reactivity and selectivity.[69] Support for this can be found in a study of $Ru_4(H)_4(CO)_{12}$ and $AuRu_4(H)_3(CO)_{12}(PPh_3)$,[38] which demonstrated that the gold adduct is significantly more active and selective than the parent complex for the catalytic isomerization of 1-pentene at 35 °C.

Preliminary results indicate that $[AuRu(H)_2(CO)(PPh_3)_4]PF_6$ (**3**) is a catalyst for the isomerization of 1-hexene to cis- and trans-2-hexene in CH_2Cl_2 at 25 °C and 1 atm of N_2. A comparison of the rate of isomerization for this complex to that of $Ru(H)_2(CO)(PPh_3)_3$ shows that the gold adduct displays an in-

(69) Braunstein, P.; Rosé, J. In *Stereochemistry of Organometallic and Inorganic Compounds*; Bernal, I., Ed.; Elsevier: Amsterdam, 1988; Vol. 3.

crease in the rate over that of the parent complex. Along with the increase in rate, a change in selectivity for the isomerization reaction was observed. The gold adduct is more selective for the production of *trans*-2-hexene while the parent is more selective for *cis*-2-hexene. It is not known why the gold changes the activity and selectivity, but work is in progress to gain a better understanding of this isomerization reaction. Analysis of the other five complexes discussed in this paper did not show evidence for catalytic activity in the isomerization of 1-hexene under similar conditions over a 24-h period.

Acknowledgment. This work was supported by the National Science Foundation (Grant CHE-851923) and the donors of the Petroleum Research Fund, administered by the American Chemical Society. We gratefully acknowledge the Johnson Matthey Co. for a generous loan of gold and iridium salts. B.D.A. also thanks General Electric Co. and the University of Minnesota Graduate School for fellowships.

Supplementary Material Available: Figures S1 and S2, displaying the ORTEP drawings of **1** and **3**, a complete table of crystal data and data collection parameters, Tables S1-S8, listing general temperature factor expressions, final positional and thermal parameters for all atoms including those of the solvate molecules, calculated hydrogen atom positions and thermal parameters, distances and angles, and least-squares planes (39 pages); Tables S9 and S10, listing observed and calculated structure factor amplitudes (79 pages). Ordering information is given on any current masthead page.

Contribution from the Department of Chemistry and the Center for Organometallic Research, University of North Texas, Denton, Texas 76203-5068

Octahedral Metal Carbonyls. 63.[1] Chelate Ring Displacement of DTHp from *cis*-(DTHp)W(CO)$_4$ by Lewis Bases (DTHp = 2,2,6,6-Tetramethyl-3,5-dithiaheptane, Lewis Base = L (Phosphine, Phosphite))

Gerard R. Dobson* and José E. Cortés

Received April 14, 1988

Reactions of *cis*-(DTHp)W(CO)$_4$, in which DTHp forms a four-membered chelate ring, with L (DTHp = 2,2,6,6-tetramethyl-3,5-dithiaheptane; L = P(OMe)$_3$, P(O-*i*-Pr)$_3$, P(OPh)$_3$, P(OCH$_2$)$_3$CCH$_3$, P(*n*-Bu)$_3$) in chlorobenzene (CB) proceed via displacement of DTHp according to *cis*-(DTHp)W(CO)$_4$ + 2L → *cis*- and *trans*-(L)$_2$W(CO)$_4$ + DTHp. Kinetics data in CB indicate the reaction to be biphasic, with *cis*-(L)(η^1-DTHp)W(CO)$_4$ present as a predominant species during the reaction's course; this intermediate has been characterized for L = P(OCH$_2$)$_3$CCH$_3$. In contrast to results observed for related systems containing five- and six-membered chelating rings, evidence here suggests that significant L-W bond making takes place in the transition states leading to chelate ring opening and closing. This conclusion is supported by activation parameters both for chelate ring opening and for chelate ring closure after pulsed laser flash photolysis in 1,2-dichloroethane (DCE) and bromobenzene (BB) solvents (solv), which generates *cis*-[(solv)(η^1-DTHp)W(CO)$_4$]; evidence suggests that this intermediate is not produced thermally. The *cis*-(L)(η^1-DTHp)W(CO)$_4$ products produced via the first phase of the biphasic thermal process undergo unimolecular W-S bond fission. Rate constants for this process vary significantly and are largely influenced by the steric properties of coordinated L, increasing in the order of larger Tolman cone angles. This W-S bond dissociation is followed by solvation to afford *cis*-[(CB)(L)W(CO)$_4$] intermediates, previously characterized, which then react via rapid reversible desolvation and attack at the five-coordinate, square-pyramidal [(L)W(CO)$_4$] intermediates by L, to afford *cis*-(L)$_2$W(CO)$_4$. Subsequent nondissociative isomerization of this species forms the equilibrium mixture of *cis*- and *trans*-(L)$_2$W(CO)$_4$ products ultimately obtained. These several steps involved in the overall chelate displacement process are discussed in detail.

Thermal displacement by phosphines and phosphites (L) of chelating ligands S_2 (S_2 = DTO = 2,2,7,7-tetramethyl-3,6-dithiaoctane, $(CH_3)_3CSCH_2CH_2SC(CH_3)_3$) and DTN (DTN = 2,2,8,8-tetramethyl-3,7-dithianonane, $(CH_3)_3SCH_2CH_2CH_2SC(CH_3)_3$), which form five- and six-membered chelating rings, respectively

cis-(S_2)W(CO)$_4$ + 2L → *trans*- and *cis*-(L)$_2$W(CO)$_4$ + S_2 (1)

has been studied extensively.[2,3] Rate data for the initial ring-opening process were interpreted in terms of a predominant dissociative mechanism, (2).[4] The results were of particular interest because, contrary to the expectation that chelate ring closure should be much faster than bimolecular interaction of L with **2b**; i.e., $k_{-a} \gg k_b$,[5] these two pathways were found to be competitive at readily accessible concentrations of L (ca. 0.1-1 M). Thus, nonlimiting rate behavior was observed, and it was possible to evaluate "competition ratios", k_b/k_{-a}, for reaction of **2b** via attack by L and by chelate ring closure. Since rates of chelate ring reclosure are independent of the identity of L, the selectivity of **2b** among various L species thus could be evaluated.[2,3]

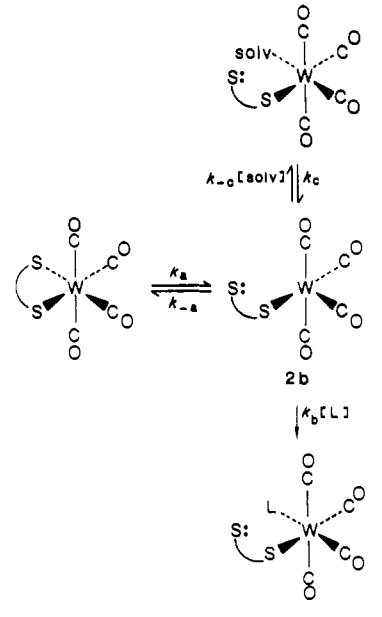

(2)

(1) Part 62: Asali, K. J.; Basson, S. S.; Tucker, J. S.; Hester, B. C.; Cortés, J. E.; Awad, H. H.; Dobson, G. R. *J. Am. Chem. Soc.* **1987**, *109*, 5386.
(2) (a) Dobson, G. R. *Inorg. Chem.* **1969**, *8*, 90. (b) Schultz, L. D.; Dobson, G. R. *J. Organomet. Chem.* **1976**, *124*, 19.
(3) (a) Dobson, G. R.; Faber, G. C. *Inorg. Chim. Acta* **1970**, *4*, 87. (b) Dobson, G. R.; Schultz, L. D. *J. Organomet. Chem.* **1977**, *131*, 285.
(4) It has recently been demonstrated[1] that replacement of CB solvent by piperidine from the closely related complex *cis*-[(CB)(P(O-*i*-Pr)$_3$)W(CO)$_4$] is dissociative; it therefore will be assumed, initially (however, see the discussion below), that replacement of solvent by L in *cis*-[(CB)(η^1-DTHp)W(CO)$_4$] intermediates also is dissociative, as is shown in eq 2.
(5) Schwarzenbach, G. *Helv. Chim. Acta* **1952**, *35*, 2344.

0020-1669/88/1327-3308$01.50/0